

WellBeing International

## WBI Studies Repository

12-2002

# Description of a Poorly Differentiated Carcinoma Within the Brainstem of a White Whale (*Delphinapterus leucas*) From Magnetic Resonance Images and Histological Analysis

Sam H. Ridgway

*Navy Marine Mammal Program*

Lori Marino

*Emory University*

T. P. Lipscomb

*Armed Forces Institute of Pathology*

Follow this and additional works at: [https://www.wellbeingintludiesrepository.org/acwp\\_vsm](https://www.wellbeingintludiesrepository.org/acwp_vsm)



Part of the [Animal Studies Commons](#), [Other Animal Sciences Commons](#), and the [Other Veterinary Medicine Commons](#)

---

### Recommended Citation

Ridgway, S. H., Marino, L., & Lipscomb, T. P. (2002). Description of a poorly differentiated carcinoma within the brainstem of a white whale (*Delphinapterus leucas*) from magnetic resonance images and histological analysis. *The Anatomical Record*, 268(4), 441-449.

This material is brought to you for free and open access by WellBeing International. It has been accepted for inclusion by an authorized administrator of the WBI Studies Repository. For more information, please contact [wbisr-info@wellbeingintl.org](mailto:wbisr-info@wellbeingintl.org).



# Description of a Poorly Differentiated Carcinoma Within the Brainstem of a White Whale (*Delphinapterus leucas*) From Magnetic Resonance Images and Histological Analysis

S.H. Ridgway<sup>1</sup>, L. Marino<sup>2</sup>, and T.P. Lipscomb<sup>3</sup>

<sup>1</sup> U.S. Navy Marine Mammal Program

<sup>2</sup> Emory University

<sup>3</sup> Armed Forces Institute of Pathology

## KEYWORDS

**white whale, magnetic resonance imaging, brainstem, tumor**

## ABSTRACT

*In this study we used magnetic resonance imaging (MRI) to investigate neuroanatomical structure in the brain of a white whale (*Delphinapterus leucas*) that died from a large tumor within the brainstem. This specimen was also compared with a normal white whale brain using MRI. MRI scans of the white whale specimen show how the tumor deformed surrounding brain structure. Histopathological analysis indicated a poorly differentiated carcinoma of uncertain origin. These analyses demonstrate the usefulness of supplementing histological analyses of pathology with studies of gross morphology facilitated by MRI.*

Cetaceans (dolphins, porpoises, and whales) exhibit a combination of neuroanatomical features that have captured the interest of many investigators. One of the more striking of these is the large absolute and relative size of the cetacean brain, which in many species equals, and in some cases exceeds, that of primates (Pilleri and Busnel, 1969; Ridgway, 1986; Worthy and Hickie, 1986; Ridgway and Tarpley, 1996; Marino, 1998). Despite comparability in size, cetacean brains exhibit many structural and organizational features that are distinct from most other mammals (Morgane et al., 1980; Ridgway, 1986; Glezer et al., 1988). Therefore, the study of cetacean brains provides valuable comparative data about the structure of large mammalian brains.

Although the morphology of the adult brain in a few cetacean species has been described (Ries and Langworthy, 1937; Kojima, 1951; Breathnach, 1960; Jansen and Jansen, 1969; Pilleri and Gihl, 1970; Jacobs et al., 1979; Morgane et al., 1980; Ridgway, 1990; Tarpley and Ridgway, 1994; Marino et al., 2001a, b), only three studies to date have taken advantage of recent neuroimaging methods to elucidate structural organization in the cetacean brain (Marino et al., 2001a–c). One of the main advantages of using neuroimaging techniques is the fact that the brain can be kept intact during examination. Therefore, the organizational structure of the various regions of interest can be maintained while the brain remains preserved for further study. This is a crucial advantage in any neuroanatomical study, but is particularly so for the study of lesser known taxonomic groups, such as cetaceans, in which the brain is organized very differently from that of other mammals. A second advantage of neuroimaging techniques is that they

allow one to visualize and measure structures and regions of interest in several spatial planes, thereby providing a way to verify measurements taken in one plane by comparing them with measurements taken in another. Third, the myriad of computer-guided software programs and image processing packages that are an integral part of neuroimaging methods arguably can provide a better degree of precision and reliability of measurement than traditional histological methods.

**Fig. 1. a and b:** Dorsal and ventral views of an intact white whale brain specimen.

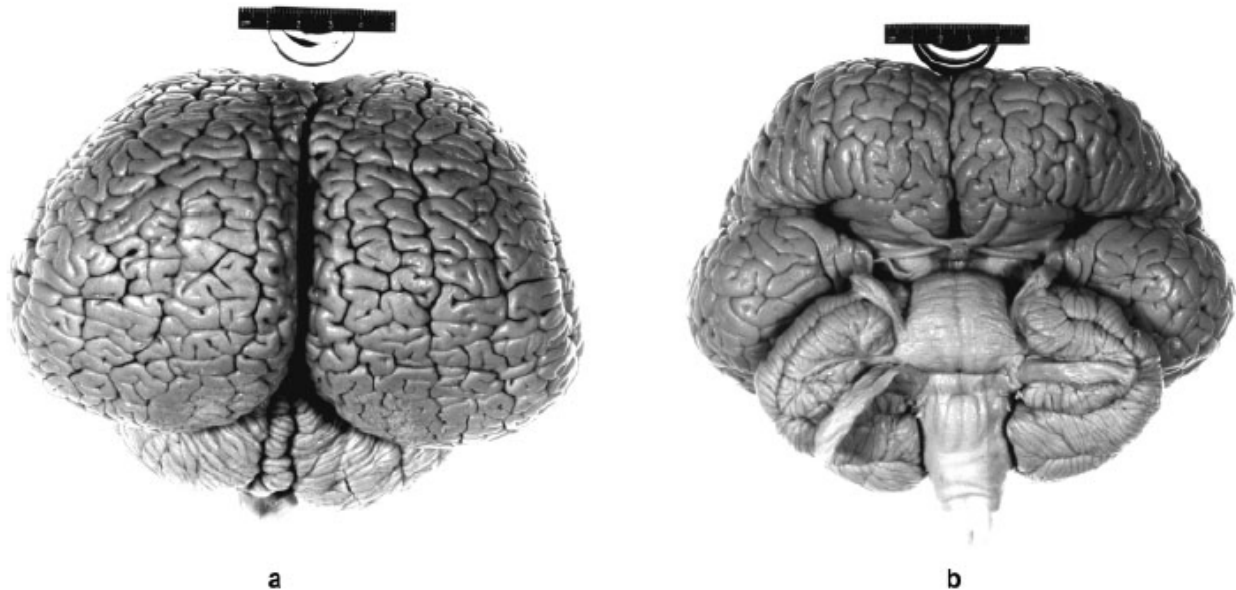


**Fig. 2. a and b:** Parasagittal sections of the left and right halves of the white whale brain specimen.



In addition to the basic comparative neuroanatomical knowledge that can be gained from using neuroimaging methods to examine cetacean brains, these techniques can also elucidate neuroanatomical abnormalities and pathologies, concerning which there is an extreme need for further studies. Tumors in cetacean brains have rarely been detected, and never in a white whale (*Delphinapterus leucas*) of the superfamily Delphinoidea. Tumors have been reported in various cetacean species (Ridgway, 1972;

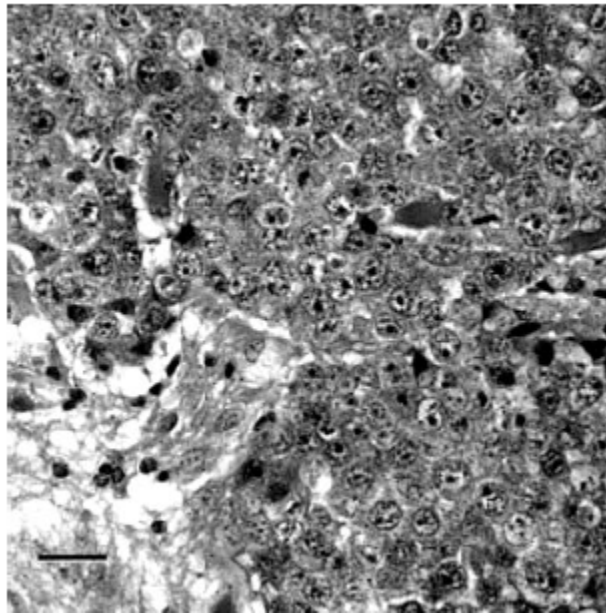
Geraci, 1987) mainly as a result of necropsy examinations of stranded animals and of observations made during whaling expeditions before 1972. However, more tumors in general (including malignant tumors) have been reported in the white whale than in any other species (De Guise et al., 1994; Martineau et al., 1994, 1995). In this study we used magnetic resonance imaging (MRI) to investigate neuroanatomical structure in the brain of a white whale that died from a large neoplasm within the brainstem. This specimen was also compared with MRI scans of a normal white whale brain from the same species as described in Marino et al. (2001a).

## MATERIALS AND METHODS

### *Specimen*

The subject of this investigation was a male white whale (*Delphinapterus leucas*) collected as an adult in July 1977 at Churchill, Manitoba, Canada, and transported to the facilities of the U.S. Marine Mammal Program in San Diego, California, where it was trained for research on sonar or echolocation. In 1983 it was moved to the program's Hawaii Center for studies at a laboratory site especially constructed for studies of whale sonar (Au et al., 1985; Penner et al., 1986; Turl et al., 1987). In late 1984 the whale became ill with an apparent chronic infection and was moved back to San Diego. White blood cell counts ranged as high as 31,000 and the animal's appetite was irregular. It was treated with various antibiotic regimes for 2–4 weeks at a time. Only temporary improvement was achieved between each course of treatment. The animal continued to lose weight. For diagnostic tests, the whale was removed from the water, whereupon it ceased breathing and died despite attempts to resuscitate it for 30 min with an endotracheal tube in place.

**Fig. 3.** H&E-stained histologic section of the brainstem from the white whale. A sheet of poorly differentiated malignant epithelial cells. The preexisting neuropil is at lower left. Bar = 25  $\mu$ m.



### *Brain Fixation and Preparation*

Necropsy examination was begun within 1 hr after death. The brain was removed, weighed fresh, and placed in 10% buffered formalin. After 6 weeks the brain was fixed sufficiently for handling. At that time the dura was removed to prepare the brain for photography (Fig. 1a and b). Upon removal of the dura and

meninges, the brainstem appeared enlarged compared to other delphinoid brains that we had observed. Because of the brainstem enlargement, we elected to preserve the specimen before sectioning for gross and histopathological examination until such time that nondestructive examination by MRI was possible.

**Fig. 4. a–h:** Coronal plane MRI sections displaying the full postero-antero extent of the tumor with major structures labeled (D = dorsal, V = ventral, R = right, L = left).

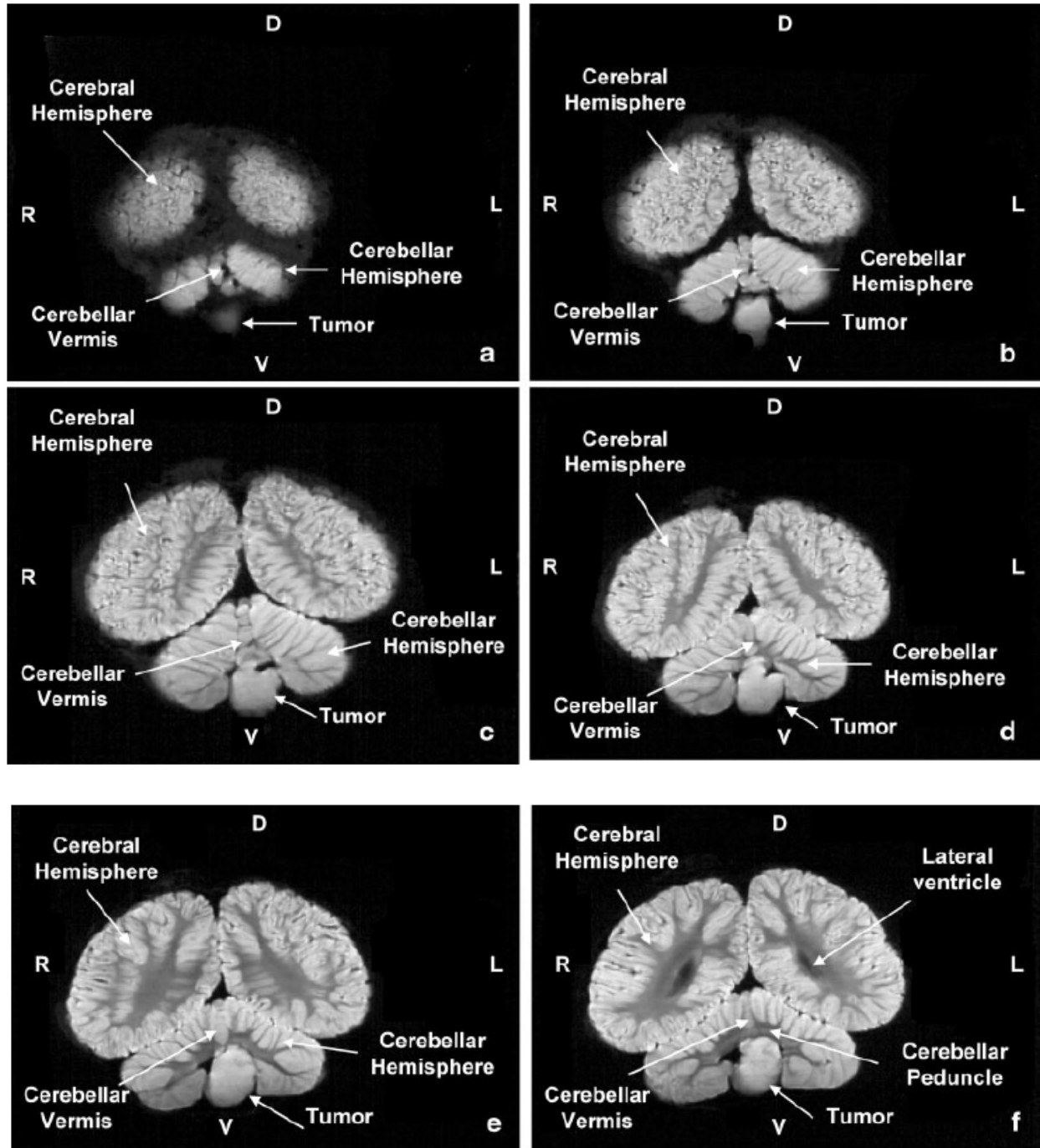
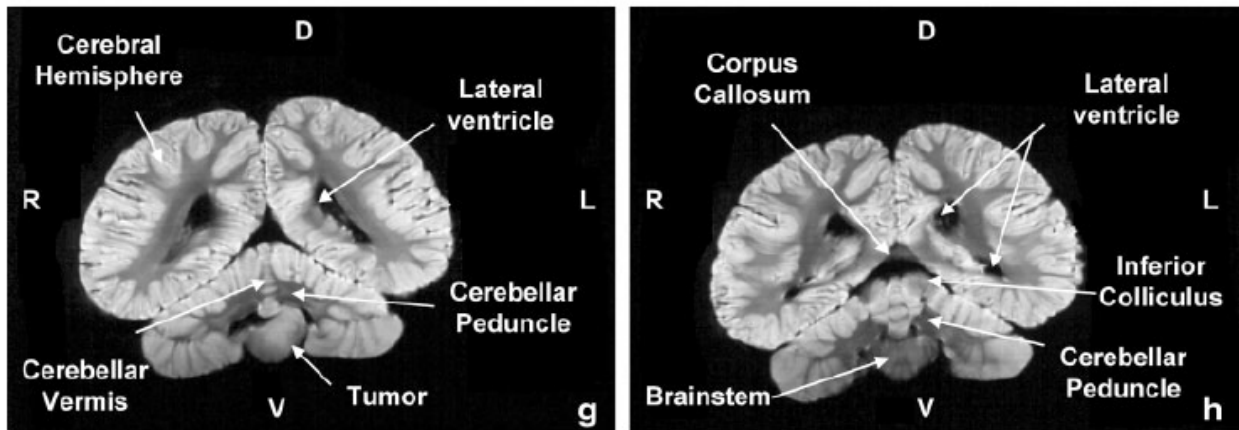


Figure 4. (continued)



#### *MRI Protocol*

After 6 years of immersion in formalin, the brain was subjected to MRI using a Siemens scanner (Siemens Medical Systems, South Iselin, NJ) with a 1.5 T magnet. The brain, still wrapped in gauze, was placed with the ventral side down in a human head coil for imaging. Because of the high level of fixation there was no distortion of the brain or tumor by placing the ventral side down in the scanner. Coronal images (5 mm thick) of the brain were acquired, and horizontal and sagittal sections (5 mm thick) were digitally reconstructed from the original images. **Volumetric Measurements** Whole brain and brainstem tumor volumes were measured from the MRI scans with Scion IMAGE, a PC-based image analysis software program. Manually-defined areas from successive slices were integrated to arrive at volume estimates. Because a certain degree of shrinkage occurs in formalin-fixed brain tissue, the proportion of the tumor to the whole-brain volume was calculated. Proportional measurements are less likely to be significantly affected by overall shrinkage.

#### *Histological Analyses*

After scanning, formalin-fixed tissue from the tumor was routinely processed, embedded in paraffin wax, and sectioned at 5  $\mu$ m. Sections were stained with hematoxylin and eosin (H&E). The avidin-biotin-peroxidase complex method (Hsu et al., 1981) was applied to deparaffinized sections using mouse monoclonal antibodies to neuron specific enolase, 1:800 dilution; mouse anti-cytokeratin, 1:1,000 dilution (Dako Laboratories, Carpinteria, CA); rabbit monoclonal antibody anti-glial fibrillary acidic protein, 1:500 dilution (Vector Laboratories, Burlingame, CA); and mouse monoclonal antibody anti-vimentin, 1:2,000 dilution (Biogenex Laboratories, San Ramon, CA). The secondary antibody was biotinylated mouse or rabbit IgG, and the detection system was a Vectastain Elite ABC kit (Vector Laboratories, Burlingame, CA). Appropriate tissues containing the antigen of interest were stained in parallel to serve as positive controls. Sections of tumor identical conditions with normal rabbit or normal mouse sera to serve as negative controls. The slides were counterstained with Mayer's hematoxylin.

#### *Normal White Whale Brain*

The normal white whale brain used for comparison was the fixed post-mortem brain of an adult female white whale that died of natural causes. Images of the entire brain were acquired with the ventral side down in the coronal plane (slice thickness = 1.3 mm) and digitally reconstructed into sagittal and horizontal images (0.94 mm thick). See Marino et al. (2001a) for a full detailed description of this specimen and methods of preparation, imaging, and analysis.

**Fig. 5.** Coronal MRI section of a normal adult white whale brain within the same postero-anterior range as displayed in Figure 4a–h.

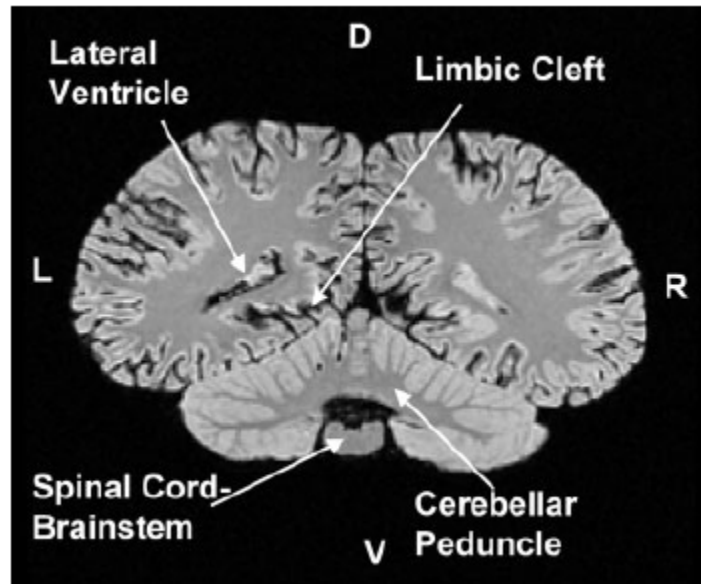


**Fig. 6. a–h:** Horizontal plane MRI sections displaying the full ventro-dorsal extent of the tumor with major structures labeled (P = posterior, A = anterior).

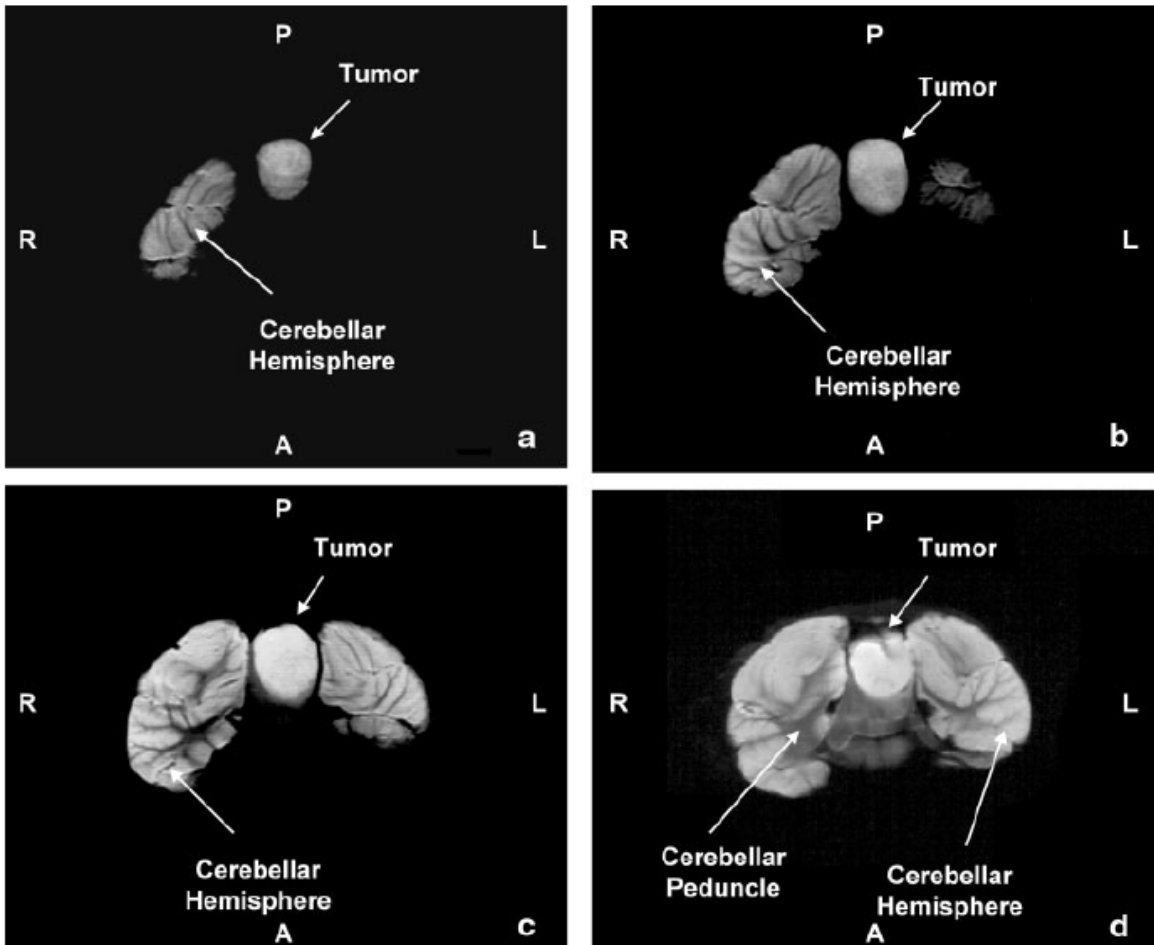
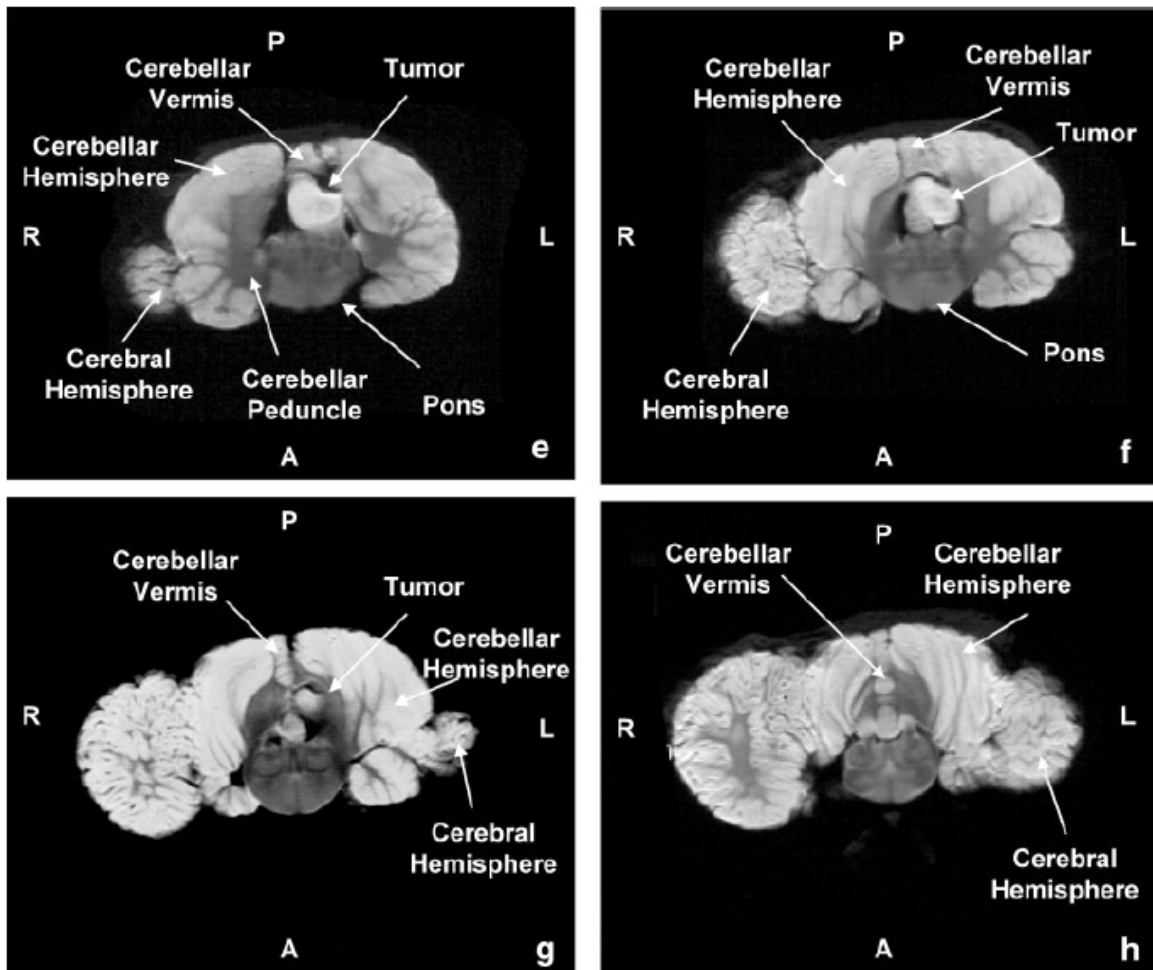


Figure 6. (continued)



## RESULTS

### *Histopathological Analysis*

Parasagittal sectioning of the brain revealed a large brainstem tumor (Fig. 2a and b). Microscopic examination of H&E-stained sections of the brainstem revealed an infiltrative neoplasm composed of polygonal cells arranged in sheets and cords (Fig. 3). The cells had distinct borders and moderate amounts of lightly eosinophilic granular to microvacuolated cytoplasm. The nuclei had coarse chromatin and one or two deeply eosinophilic nucleoli. Mitotic figures were numerous, and there were multifocal areas of necrosis that contained mineralized debris.

Immunohistochemical stains for glial fibrillary acidic protein (a marker for glial cells), neuron-specific enolase (a marker for neurons and various other cells), and vimentin (a marker for mesenchymal cells) were negative in the neoplastic cells, suggesting that the tumor was not glial, neuronal, or mesenchymal. Scattered neoplastic cells were intensely positive for cytokeratin, which is a marker for epithelial cells.

### *MRI*

Figure 4a–h shows the full extent of the tumor in the coronal plane from posterior to anterior with major structures labeled. An image of a normal adult white whale brain (from a specimen that was the subject of



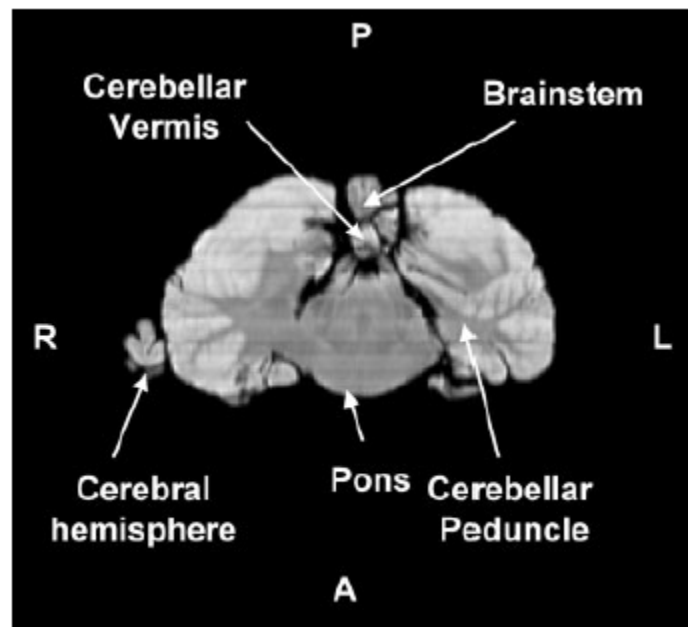
a previously published study) within the same postero-anterior range is displayed in Figure 5 for comparison. Figure 4 shows that the tumor extends laterally both left and right from midline but has displaced the left cerebellar hemisphere more so than the right cerebellar hemisphere. The mass also extends the dorso-ventral extent of the brainstem and contacts the cerebellar vermis. Figure 6a–h shows the full ventro-dorsal extent of the tumor in the horizontal plane with major structures labeled. Figure 6, particularly e–g, shows the lateral asymmetry of the tumor. Figure 7 shows the normal brain in the horizontal plane within the same dorso-ventral range.

Figure 8a–h shows the full lateral extent of the tumor in the sagittal plane from left to right with major structures labeled. Figure 8 displays the way in which the tumor produces a mass effect by extending up onto the cerebellum from the ventral side. This figure also shows that the tumor is relatively caudal in its location and extent within the brainstem. The normal brain within the same latero-medial range is shown in Figure 9.

#### *Volumetric Analysis*

Volumetric measurements of the tumor mass and whole brain were conducted. These analyses revealed that the whole brain volume was 2018.11 cc, which is not substantially different from the fresh brain weight of 2079 g if volume is converted to mass (because the specific gravity of brain tissue is close to the value of one) and is well within the normal range for an adult white whale (Ridgway and Brownson, 1984). The volume of the tumor mass was 25.75 cc, thus consisting of 1.28% of the whole brain mass.

**Fig. 7.** Horizontal MRI section of a normal adult white whale brain within the same ventro- dorsal range as displayed in Figure 6a–h.



#### **DISCUSSION**

Magnetic resonance images of the white whale specimen confirm the presence of a relatively large and well-defined mass in the brainstem. The images also show that the tumor is asymmetrical and has displaced the left cerebellar lobe more than the right. Sagittal images show that the mass has expanded anteriorly to make contact with the base of the cerebellum. Volumetric analysis of the tumor and whole brain indicate this mass has infiltrated approximately 1.3% of the whole brain volume.

The histological appearance of the cells within the tumor (cohesive polygonal cells with distinct borders) and cytokeratin positivity support an epithelial origin. On the basis of histopathologic and immunohistochemical findings, poorly differentiated carcinoma was diagnosed. The neoplasm stands out sharply from the background neuropil (the network of delicate unmyelinated nerve fibers that permeates the central nervous system) as a mass of cohesive polygonal cells with distinct borders and prominent features of malignancy, such as nuclear atypia and mitotic activity. The site of origin of the carcinoma is unknown. In humans, epidermoid cysts of the cerebellopontine angle sometimes undergo malignant transformation and give rise to carcinomas (Goldman and Gandy, 1987). Metastasis from a distant site is also possible. Neoplasia was not detected by gross or microscopic examination in other tissues from the whale.

**Fig. 8. a–h:** Sagittal plane MRI sections from left to right displaying the full lateral extent of the tumor in the sagittal plane with major structures labeled.

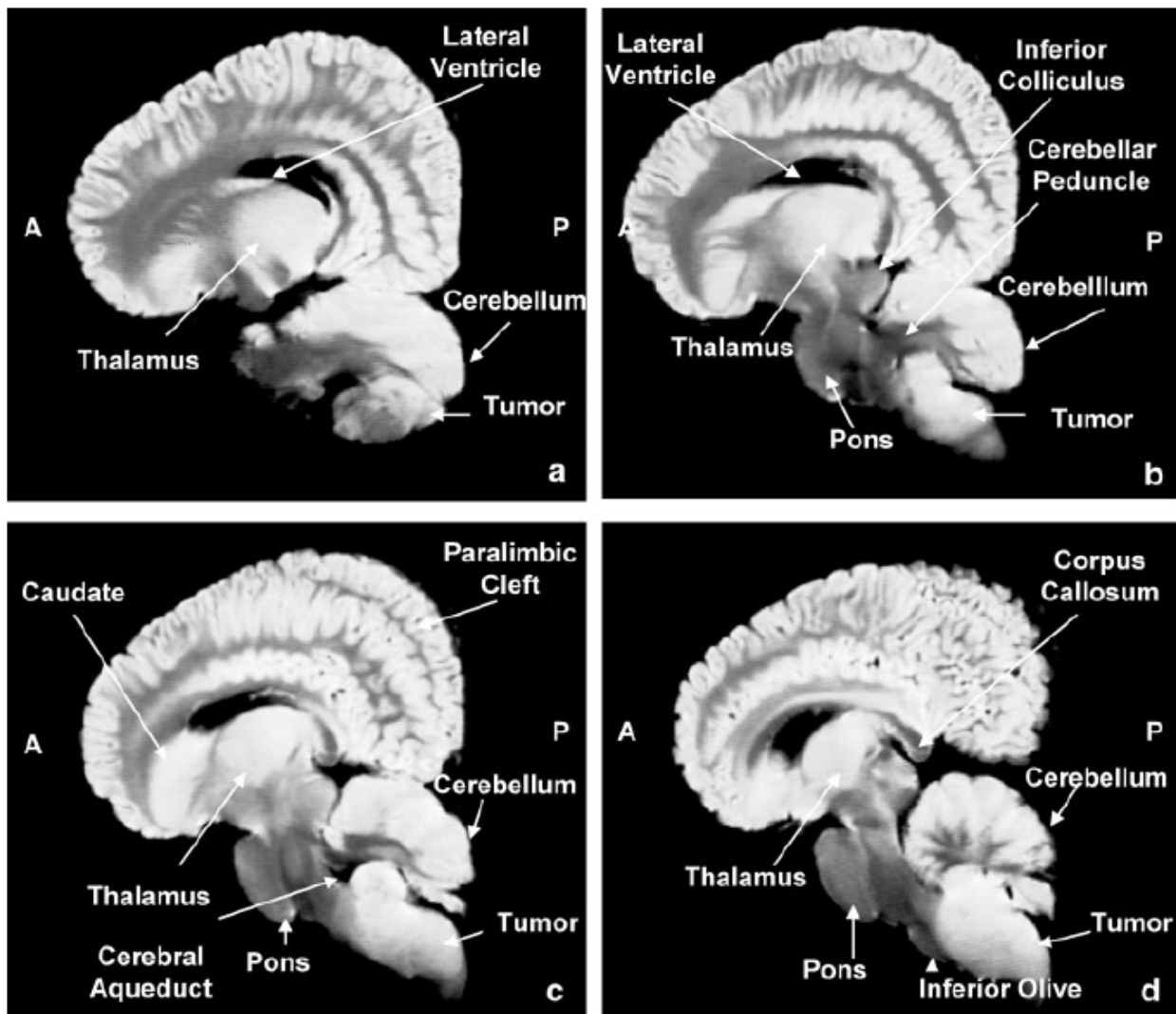


Figure 8. (continued)

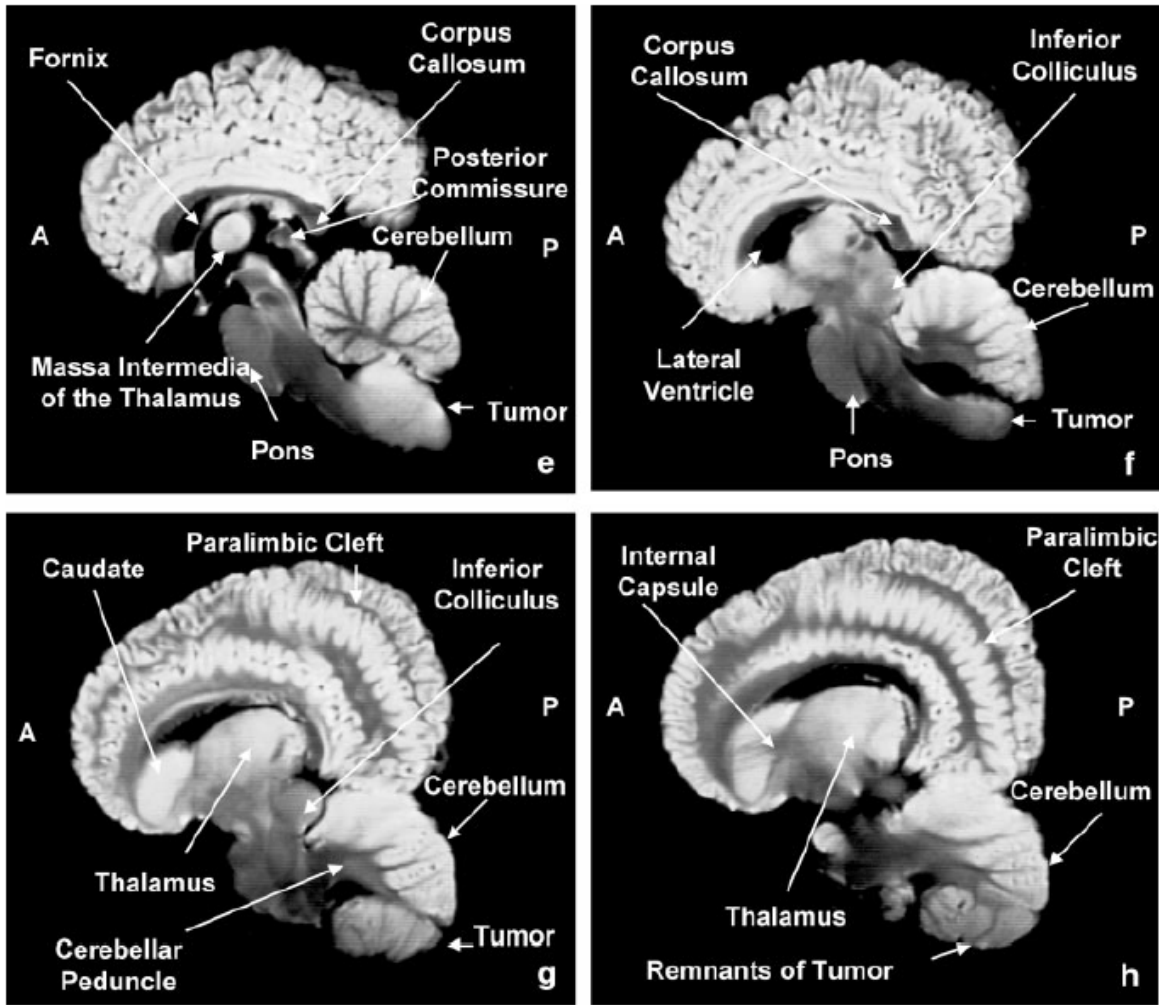
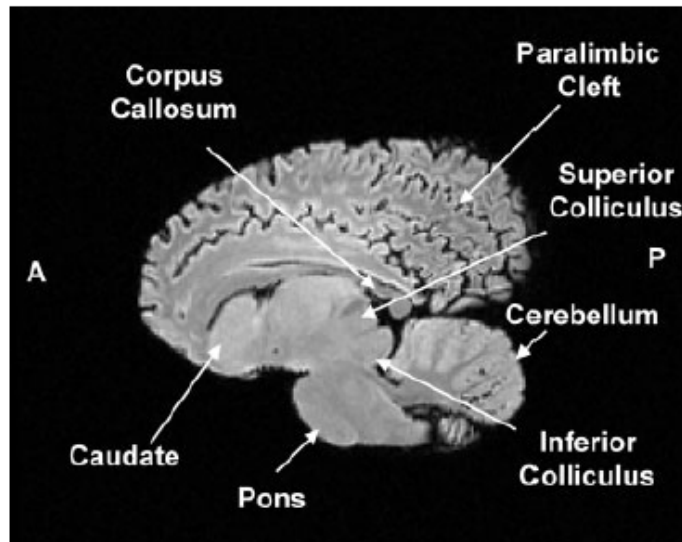


Fig. 9. Sagittal MRI section of a normal adult white whale brain within the same latero-medial range as displayed in Figure 8a-h.



This is the first brain tumor to be reported in a white whale and only the third reported in a cetacean. In a review of tumor incidence in cetaceans, Geraci (1987) listed only two tumors within the brain, both of which were from large baleen whales. By far the greatest incidence of tumors in cetaceans has been in the small St. Lawrence white whale population from Eastern Canada, where human-generated pollution has been considered to be a contributory cause (De Guise et al., 1994; Martineau et al., 1994). The brain was not listed among the tissues examined during necropsy (De Guise et al., 1994). Our specimen was from the much more numerous Hudson Bay population of white whales.

Brains from stranded cetaceans are not commonly or extensively examined. Often there is a conflict between those who want to examine the brain and those who want to preserve the skull for taxonomic examination. In these cases imaging could be employed to screen brains for tumors and other major pathologies while leaving the skull intact.

Although histological and immunohistochemical results are crucial to identifying and describing lesions, the use of MRI can add substantially to our understanding of how tumor masses affect the surrounding structures of the brain, as has been effectively demonstrated in humans and other more commonly studied species. Such information will allow for a better understanding of cetacean biology and behavior within both healthy and pathological contexts.

#### **ACKNOWLEDGMENTS**

We thank R. Buxton, K. Hickey, and C. Platenburg for assistance with scanning and data analysis for this study.

#### **LITERATURE CITED**

- Au WW, Carder DA, Penner RH, Scronce BL. 1985. Demonstration of adaptation in beluga whale echolocation signals. *J Acoust Soc Am* 77:726–730.
- Breathnach AS. 1960. The cetacean nervous system. *Biol Rev Cambr Phil Soc* 35:187–230.
- De Guise S, Lagace A, Beland P. 1994. Tumors in St. Lawrence beluga whales (*Delphinapterus leucas*). *Vet Pathol* 31:444–449.
- Geraci JR. 1987. Tumors in cetaceans: analysis and new findings. *Can J Fish Aqua Sci* 44:1289–1300.
- Glezer I, Jacobs MS, Morgane PJ. 1988. Implications of the “initial brain” concept for brain evolution in Cetacea. *Behav Brain Sci* 11:75–116.
- Goldman SA, Gandy SE. 1987. Squamous cell carcinoma as a late complication of intracerebroventricular epidermoid cyst. *Case Rep J Neurosurg* 66:618–620.
- Hsu SM, Raine L, Fanger H. 1981. Use of avidin-biotin-peroxidase complex (ABC) in immunoperoxidase techniques: a comparison between ABC and unlabeled antibody (PAP) procedures. *J Histochem Cytochem* 29:577–580.
- Jacobs MS, McFarland WL, Morgane PJ. 1979. The anatomy of the brain of the bottlenose dolphin (*Tursiops truncatus*). Rhinic lobe (rhinencephalon): the archicortex. *Brain Res Bull* 4:1–108.
- Jansen J, Jansen J. 1969. The nervous system of cetacean. In: Anderson HT, editor. *The biology of marine mammals*. London: Academic Press. p 175–252.

- Kojima T. 1951. On the brain of the sperm whale (*Physeter catadon* L.). Sci Rep Whales Res Inst Tokyo 6:49–72.
- Marino L. 1998. A comparison of encephalization between odontocete cetaceans and anthropoid primates. Brain Behav Evol 51:230–238.
- Marino L, Murphy TL, DeWeerd AL, Morris JA, Ridgway SH, Fobbs AJ, Humblot N, Johnson JI. 2001a. Anatomy and three-dimensional reconstructions of the brain of a white whale (*Delphinapterus leucas*) from magnetic resonance images (MRI). Anat Rec 262:429–439.
- Marino L, Sudheimer K, Murphy TL, Davis KK, Pabst DA, McClellan W, Rilling JK, Johnson JI. 2001b. Anatomy and three-dimensional reconstructions of the bottlenose dolphin (*Tursiops truncatus*) brain from magnetic resonance images. Anat Rec 264:397–414.
- Marino L, Murphy TL, Gozal L, Johnson JI. 2001c. Magnetic resonance imaging and three-dimensional reconstructions of the brain of the fetal common dolphin, *Delphinus delphis*. Anat Embryol 203:393–402.
- Martineau D, De Guise S, Fournier M, Shugart L, Girard C, Lagace A, Beland P. 1994. Pathology and toxicology of beluga whales from the St. Lawrence Estuary, Quebec, Canada. Past, present, and future. Sci Total Environ 154:201–215.
- Martineau D, Lair S, De Guise S, Beland P. 1995. Intestinal adenocarcinomas in two beluga whales (*Delphinapterus leucas*) from the estuary of the St. Lawrence River. Can Vet J 36:563–565.
- Morgane PJ, Jacobs MS, McFarland WL. 1980. The anatomy of the brain of the bottlenose dolphin (*Tursiops truncatus*). Surface configurations of telencephalon of the bottlenose dolphin with comparative anatomical observations in four other cetacean species. Brain Res Bull 5:1–108.
- Penner RH, Turl CW, Au WW. 1986. Biosonar detection by the beluga whale (*Delphinapterus leucas*) using surface reflected pulse trains. J Acoust Soc Am 80:1842–1843.
- Pilleri G, Busnel R. 1969. Brain/body weight ratios in Delphinidae. Acta Anat 73:92–97.
- Pilleri G, Gahr M. 1970. The central nervous system of the mysticete and odontocete whales. In: Pilleri G, editor. Investigations on cetacea. Vol II. Berne, Switzerland: Brain Anatomy Institute. p 89–127.
- Ridgway SH. 1972. Mammals of the sea: biology and medicine. Springfield: Thomas. 812 p.
- Ridgway SH, Brownson RH. 1984. Relative brain sizes and cortical surface areas in odontocetes. Acta Zool Fenn 172:149–152.
- Ridgway SH. 1986. Dolphin brain size. In: Bryden MM, Harrison RH, editors. Research on dolphins. Oxford: Oxford University Press. p 59–70.
- Ridgway SH. 1990. The central nervous system of the bottlenose dolphin. In: Leatherwood S, Reeves RR, editors. The bottlenose dolphin. San Diego: Academic Press. p 69–100.
- Ridgway SH, Tarpley RJ. 1996. Brain mass comparisons in Cetacea. Proc Int Assoc Aquat Anim Med 27:55–57.
- Ries FA, Langworthy O. 1937. A study of the surface structure of the brain of the whale (*Balaenoptera physalus* and *Physeter catadon*). J Comp Neurol 68:1–47.

Tarpley RJ, Ridgway SH. 1994. Corpus callosum size in delphinid cetaceans. *Brain Behav Evol* 44:156–165.

Turl CW, Penner RH, Au WW. 1987. Comparison of target detection capabilities of the beluga and bottlenose dolphin. *J Acoust Soc Am* 82:1487–1491.

Worthy GA, Hickie JP. 1986. Relative brain size in marine mammals. *Am Nat* 128:445–459.